The Astronomical Journal, 131:1405–1415, 2006 March

THE ANISOTROPIC DISTRIBUTION OF M31 SATELLITE GALAXIES: A POLAR GREAT PLANE OF EARLY-TYPE COMPANIONS

Andreas Koch and Eva K. Grebel
Department of Physics and Astronomy, Astronomical Institute of the University of Basel, Venusstrasse 7, CH-4102 Binningen, Switzerland; koch@astro.unibas.ch
Received 2005 August 3; accepted 2005 November 8

ABSTRACT

The highly anisotropic distribution and apparent alignment of the Galactic satellites in polar great planes begs the question of how common such distributions are. The satellite system of M31 is the only nearby system for which we currently have sufficiently accurate distances to study the three-dimensional satellite distribution. We present the spatial distribution of the 15 currently known M31 companions in a coordinate system centered on M31 and aligned with its disk. Through a detailed statistical analysis we show that the full satellite sample describes a plane that is inclined by -56° with respect to the poles of M31 and has an rms height of 100 kpc. At 88% the statistical significance of this plane is low, and it is unlikely to have a physical meaning. We note that the great stellar stream found near Andromeda is inclined to this plane by 7°. Most of the M31 satellites are found within $<\pm 40^\circ$ of M31's disk; i.e., there is little evidence for a Holmberg effect. If we confine our analysis to early-type dwarfs, we find a best-fit polar plane within 5°–7° from the pole of M31. This polar great plane has a statistical significance of 99.7% and includes all dSphs (except for And II), M32, NGC 147, and PegDIG. The rms distance of these galaxies from the polar plane is 16 kpc. The nearby spiral M33 has a distance of only $\sim$3 kpc from this plane, which points toward the M81 group. We discuss the anisotropic distribution of M31's early-type companions in the framework of three scenarios, namely, as remnants of the breakup of a larger progenitor, as a tracer of a prolate dark matter halo, and as a tracer of collapse along large-scale filaments. The first scenario requires that the breakup must have occurred at very early times and that the dwarfs continued to form stars thereafter to account for their stellar population content and luminosity-metallicity relation. The third scenario seems to be plausible, especially when considering the apparent alignment of our potential satellite filament with several nearby groups. The current data do not permit us to rule out any of the scenarios. Orbit information is needed to test the physical reality of the polar plane and of the different scenarios in more detail.

Key words: galaxies: dwarf — galaxies: evolution — galaxies: individual (M31, M32, M33, NGC 147, NGC 185, NGC 205, Andromeda I, II, III, V, VI, VII, IX, PegDIG) — galaxies: interactions — galaxies: kinematics and dynamics — Local Group

Online material: color figures

1. INTRODUCTION

The galaxies of the Local Group are not randomly distributed but exhibit a number of distinct patterns. First, there is a pronounced morphology-density relation. Gas-poor late-type dwarf galaxies are mainly found in close proximity to one of the two dominant spiral galaxies in the Local Group, the Milky Way and M31. Typically, these dwarfs have distances of less than 300 kpc from the closest spiral galaxy and comprise dwarf elliptical and dwarf spheroidal galaxies (dEs and dSphs, respectively). Gas-rich early-type dwarf galaxies (primarily dwarf irregular galaxies [dIrrs] but also so-called transition-type dIrr/dSphs; see Grebel et al. [2003] for details), on the other hand, show a less concentrated distribution and are also common at larger distances (e.g., Fig. 3 in Grebel [1999] and Fig. 1 in Grebel [2000]). Second, the satellites of the Milky Way show an anisotropic distribution in the sense that locations around the polar axis, well away from the Galactic plane, are preferred, resembling the Holmberg effect (Holmberg 1969). Third, the companions of the Milky Way and some of the outer halo globular clusters lie close to one or two polar great planes (e.g., Lynden-Bell 1976, 1982; Kunkel & Demers 1976; Kunkel 1979; Majewski 1994; Fusi Pecci et al. 1995; Kroupa et al. 2005). There may be additional "streams" comprising only one or a few satellites and outer halo globular clusters (e.g., Lynden-Bell & Lynden-Bell 1995; Palma et al. 2002).

It is curious that essentially all of the Milky Way satellites appear to be located in one or two great planes. A number of studies showed that the probability of such planar alignments to have occurred by chance is very low (e.g., Kunkel 1979; Kroupa et al. 2005). Several suggestions were put forward to explain the nonisotropic, planar distribution of the satellites. According to one of these scenarios, the Galactic satellites may be remnants of one or two larger, disrupted galaxies and orbit the Milky Way within the great planes defined by their original parents (e.g., Kunkel 1979; Lynden-Bell 1982; Palma et al. 2002). Whether the orbits of all these satellites do indeed lie within the planes is at present still unclear. For some, the proper motions seem to agree with motion within the plane of apparent alignment, whereas this is apparently ruled out for other objects (e.g., Schweitzer et al. 1995, 1997; Dauphole et al. 1996; Grebel 1997; Palma et al. 2002; Piatek et al. 2002, 2003, 2005; Dinescu et al. 2004). However, the uncertainties of the proper-motion measurements are at present still uncomfortably large, and we will have to await more accurate measurements with forthcoming astrometric space missions such as ESA's *Gaia* and NASA's *Space Interferometry Mission*. Another scenario suggests that satellites follow their massive host's dark matter distribution. Kang et al. (2005)

demonstrate that in this case satellites may exhibit planar distributions as observed for the Milky Way satellites, although they find a distribution almost perpendicular to the stellar Galactic plane to be unexpected. Hartwick (1996, 2000) argues that the Galaxy's dark halo has "an extended prolate triaxial distribution highly inclined to the Galactic plane," thus accounting for the satellites' polar alignment. In a third, related scenario Knebe et al. (2004) suggest that satellites retain the alignment with the massive primary that they had when they first fell into the group or cluster along a filament. Zentner et al. (2005) and Libeskind et al. (2005) point out that cold dark matter (CDM) hierarchical structure formation scenarios lead to highly anisotropic collapse along filaments, naturally resulting in planar configurations aligned with the major axis of the dark matter distribution. Both groups share the view that the Galactic stellar disk should be approximately perpendicular to the major axis of the dark matter distribution, an orientation supported by recent disk galaxy formation simulations (Navarro et al. 2004) that may also provide a natural explanation for the Holmberg effect. All these scenarios have one idea in common: they all suggest that the planar alignment reflects the plane of motion of the satellites.

Is the Milky Way exceptional in having its satellites located in one or two great planes? If such alignments are common, are they preferentially polar? If one or several of the above scenarios hold, then similar great planes (possibly even polar great planes) should also be found for the satellite systems of other galaxies. The Holmberg effect in itself is not a sufficient criterion for the existence of polar planes, since (with the exception of the Milky Way's surroundings) the observational evidence for it comes from the *projected* distribution of (often very few) satellites around distant primaries. Furthermore, there is some debate as to whether the Holmberg effect really exists (compare, e.g., Sales & Lambas [2004] and Brainerd [2005]). If great planes generally exist, this would reveal the orbital planes of the satellite galaxies, would help to elucidate the origin of the satellites, and could help us understand the accretion history of massive galaxies.

We can investigate these questions by turning to our next closest spiral galaxy, M31. M31 has a satellite system that covers the same range of distances as the Galactic satellites. Moreover, the distances of these satellites have been well-determined using mainly observations with the *Hubble Space Telescope* (*HST*). In particular, for the majority of these satellites heliocentric distances are available that were measured using a combination of several distance indicators such as the tips of the red giant branch and the horizontal branch, permitting one to derive deprojected distances of these dwarf galaxies from M31 with some confidence (see Grebel [2000] and Grebel et al. [2003], Table 1). This allows us to use the three-dimensional galaxy distribution and to search for possible planes.

M31 is surrounded by three dEs and one dwarf-sized compact elliptical galaxy (cE; namely, M32). It has at least seven dSph companions, four of which were only discovered and confirmed during the last few years (Armandroff et al. 1998, 1999; Karachentsev & Karachentseva 1999; Grebel & Guhathakurta 1999; Zucker et al. 2004b; Harbeck et al. 2005). Additional very faint satellites may yet be uncovered. Furthermore, M31 contains one dIrr and one dIrr/dSph within 300 kpc and two more such dwarfs within a radius of 500 kpc. Altogether there are 13 satellites known within 300 kpc and 15 satellites within 500 kpc whose spatial distribution can be investigated.

The first search for possible great planes in the distribution of M31 satellites was conducted by Grebel et al. (1999), who at that time had primarily ground-based distance determinations at their disposal. They found that seven (possibly eight) of 13 satellites appeared to lie within $\pm 15^\circ$ of a great plane around M31, with a probability for chance alignment of $\leq 5\%$. M33 seemed to lie near an extension of this plane. Grebel et al. (1999) saw little evidence for a Holmberg effect in the distribution of M31's companions.

In the current paper we carry out a more sophisticated analysis using improved statistical tools and largely homogeneous *HST* distances wherever available. Distances derived from *HST* photometry are preferred owing to their superior seeing, resolution, and depth and because several distance indicators were often combined in determining the distances. This paper is organized as follows: Section 2 introduces the method used to define a native coordinate system (CS) aligned with the host galaxy M31. In § 3 the procedure of determining the best-fit planes and performing statistical tests is presented together with the resulting planes, and in § 4 we turn to the special subgroup of M31's early-type satellites. Finally, § 5 discusses the results in terms of dynamical aspects of M31's accretion history and cosmological substructure populations. Section 6 then summarizes our findings.

2. THE DEFINITION OF A NATIVE M31 COORDINATE SYSTEM

In order to determine the positions of the M31 satellites relative to M31, we define an absolute CS that is anchored to the center of M31 and has two of its vectors lying in the disk plane of M31. Coordinates and distances were taken from Zucker et al. (2004b) and Harbeck et al. (2005) for And IX and from Grebel et al. (2003) and Grebel (2000) for the remaining galaxies. First, each pair of J2000.0 equatorial coordinates (α, δ) was converted into Galactic longitude and latitude (l, b), and from that three-dimensional Cartesian (x, y, z) positions relative to the Sun were calculated,

$$\begin{aligned} x &= D_\odot \cos b \cos l, \\ y &= D_\odot \cos b \sin l, \\ z &= D_\odot \sin b, \end{aligned} \tag{1}$$

where $D_\odot$ denotes the observed distances from the Sun (see Table 1). This right-handed CS (eq. [1]) is oriented such that x points toward the Galactic center and z indicates the height above the Galactic plane.

After applying a linear translation to move the origin of this CS to the center of M31, the CS is aligned with this galaxy by rotation around three angles. The first of these affine transformations incorporates the position angle (P.A.) of M31. Accounting for the inclination of the celestial against the Galactic pole and M31's P.A. of $37\overset{\circ}{.}7 \pm 0\overset{\circ}{.}2$ (de Vaucouleurs 1958), we rotate the CS clockwise using a transpose rotation matrix around the y-axis,[1] $R_y^T(p)$, by the angle $p = 115\overset{\circ}{.}17$. In the next step, the resulting CS is rotated around the new x-axis by inclination via the matrix $R_x^T(i)$, where we use the canonical value for the inclination of M31 of $i = -12\overset{\circ}{.}5$ (de Vaucouleurs 1959). In this notation, 90° signifies a face-on view. The minus sign arises because the matrices are defined for clockwise rotation. Finally, we rotate the resulting CS, which is now coplanar with the M31 galactic plane, around its respective z-axis by 180° by means of $R_z^T(\pi)$.

[1] Since we rotate the CS rather than the coordinates themselves, the transpose matrix has to be used.

TABLE 1
SATELLITE SAMPLE

Galaxy	Type	α (J2000.0)	δ (J2000.0)	$D_\odot$ (kpc)	X_{M31} (kpc)	Y_{M31} (kpc)	Z_{M31} (kpc)
M31	Spiral	00 42 44	+41 16 09	773 ± 20	0.0	0.0	0.0
M32	cE	00 42 42	+40 51 55	770 ± 40	4.7	4.0	0.1
NGC 205	dE	00 40 22	+41 41 07	830 ± 35	3.8	−55.3	16.0
And I	dSph	00 45 40	+38 02 28	790 ± 30	41.0	−0.5	24.7
And III	dSph	00 35 34	+36 29 52	760 ± 70	63.2	23.2	−7.2
NGC 147	dE	00 33 12	+48 30 29	755 ± 35	−85.5	−8.7	−52.4
And V	dSph	01 10 17	+47 37 41	810 ± 45	−104.2	−26.3	45.8
And II	dSph	01 16 30	+33 25 09	680 ± 25	42.2	144.9	53.5
NGC 185	dE	00 38 58	+48 20 12	620 ± 25	−89.3	121.6	−89.4
Cas dSph	dSph	23 26 31	+50 41 31	760 ± 70	−86.3	−50.5	−191.5
IC 10	dIrr	00 20 17	+59 18 14	660 ± 65	−200.0	70.7	−140.7
And VI	dSph	23 51 46	+24 34 57	775 ± 35	243.1	37.6	−100.5
LGS 3	dIrr/dSph	01 03 53	+21 53 05	620 ± 20	149.1	240.6	21.4
PegDIG	dIrr/dSph	23 28 36	+14 44 35	760 ± 100	355.5	106.5	−174.5
IC 1613	dIrr	01 04 47	+02 07 02	715 ± 35	369.2	334.5	84.8
And IX	dSph	00 52 53	+43 12 00	790 ± 70	−31.6	−12.4	22.0
M33	Spiral	01 33 51	+30 39 37	847 ± 60	87.4	49.8	196.7
G1	Globular cluster	00 32 47	+39 34 40	773 ± 20	29.4	−2.8	−17.4
B327	Globular cluster	00 41 35	+41 14 55	773 ± 20	1.3	−0.9	−2.5

NOTES.—Units of right ascension are hours, minutes, and seconds, and units of declination are degrees, arcminutes, and arcseconds. Coordinates and heliocentric distances are from Rich et al. (1996), Grebel (2000), Barmby et al. (2002), Grebel et al. (2003), Zucker et al. (2004b), and Harbeck et al. (2005), and X, Y, and Z coordinates are given in our Cartesian coordinate system centered on M31.

Thus, consistent with common representations, our CS is oriented such that X_{M31} increases toward the southwest, Y_{M31} increases toward the northwest, and Z_{M31} points toward M31's galactic pole.

The transformed Cartesian coordinates are thus determined from $(X_{M31},\ Y_{M31},\ Z_{M31})^T = R_z^T(\pi)R_x^T(i)R_y^T(p)(x,\ y,\ z)^T$. The expressions for the individual components are as follows:

$$\begin{aligned} X_{M31} &= -x\cos p + z\sin p, \\ Y_{M31} &= -y\cos i - x\sin i\sin p + z\sin i\cos p, \\ Z_{M31} &= y\sin i - x\cos i\sin p + z\cos i\cos p. \end{aligned} \tag{2}$$

A schematic diagram of the satellites' location relative to M31 in this native M31 CS is shown in Figure 1. The uncertainties in each of the three coordinates were derived by applying the above transformations accounting for the uncertainties in the distances as the only error source. Figure 1 (*right*) seems to suggest the absence of an obvious Holmberg effect in the satellite distribution. Furthermore, by eye one may be tempted to position a possible great circle along the approximate longitudes of +30° and −150°, but this does not look like a very well-defined great circle. Since it is difficult to determine a preferential alignment of the satellite distribution by eye, we now pursue the question of great planes

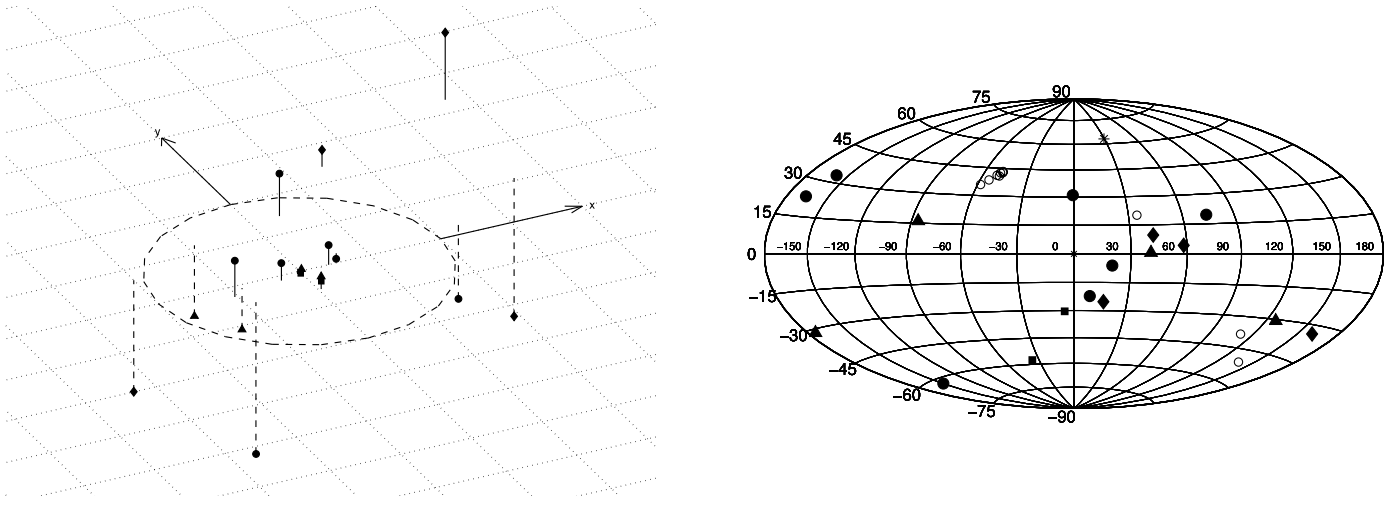

FIG. 1.—*Left*: Illustration of the position of the M31 satellites relative to the disk plane of M31. The dotted grid indicates the location of M31's disk plane, which contains the x- and y-coordinates of our coordinate system centered on M31. Solid and dashed lines indicate companion galaxies above and below this plane, respectively. The different symbols refer to the morphological types of the M31 companions: dSphs (*circles*), dEs and cEs (*triangles*), and dIrrs and dIrr/dSphs (*diamonds*). M31 itself is marked by a cross. The axes of each grid have a length of 100 kpc. The dashed circle circumscribes the central 200 kpc around M31. *Right*: Aitoff projection of the same data in the M31 reference system, also including the Andromeda Stream (*open circles*), its two most massive globular clusters (*squares*), and M33 (*asterisk*). Note the lack of an obvious Holmberg effect. Visual inspection suggests a possible great circle of satellites along the latitudes of approximately +30° and −150°. [*See the electronic edition of the Journal for a color version of this figure.*]

comprising all or subsets of M31's companions via a statistical approach.

3. GREAT PLANES INCLUDING ALL SATELLITES

The most convenient parameterization of a plane is the Hesse form, which describes each point within the plane in terms of the normal vector $\boldsymbol{n}$ and two vectors, $\boldsymbol{x}$ and $\boldsymbol{p}$, each pointing from the origin to a point located on the plane. Then $\boldsymbol{n}(\boldsymbol{x}-\boldsymbol{p})=0$ unambiguously defines the plane. One can determine the closest distance D_p between the origin of the CS and the plane via $D_p=\boldsymbol{n}\cdot\boldsymbol{p}$ (see also Kroupa et al. 2005). Since we seek to identify great circles or great planes, the plane needs to intersect the origin (i.e., the center of M31), which allows us to set D_p to zero. Then the Hesse form can be simplified as follows:

$$n_1 X_{\rm M31}+n_2 Y_{\rm M31}+n_3 Z_{\rm M31}=0. \quad (3)$$

Here n_i denotes the respective components of the plane's normal vector[2] and $(X_{\rm M31}, Y_{\rm M31}, Z_{\rm M31})$ is the position vector of each satellite, as determined above. From this the distance of any point (x_i, y_i, z_i) to the plane is given by $d_p=(n_1x_i+n_2y_i+n_3z_i)/(n_1^2+n_2^2+n_3^2)^{1/2}$. We fit the implicitly defined surface (eq. [3]) to our data by means of an error-weighted orthogonal distance regression (ODR) using ODRPACK (Boggs & Rogers 1990; Boggs et al. 1992). Instead of minimizing the projected distance to the plane in a given coordinate, as in a traditional least-squares fit, ODR takes into account the perpendicular distance to the curves to fit. The individual data points were weighted in the fit by the deprojected uncertainties in the three-dimensional positions, which were calculated from the measurement uncertainties in the galaxies' distances.

3.1. *The Best-Fit Satellite Plane*

The formally best-fit plane that we obtained by performing one single ODR fit comprising the entire sample of 15 satellites lies at a normal vector of $l=171\overset{\circ}{.}2$ and $b=-45\overset{\circ}{.}6$. However, anticipating the statistical method in § 3.3, the significance of this plane is 84%, corresponding to 1.4 Gaussian σ, and we cannot reject the possibility that such a plane is a purely random alignment. If we describe the rms height of an underlying disk distribution for N satellites as $\Delta=[(1/N)\sum_{i=1}^{N} d_p^2(i)]^{1/2}$, this value is found to be 99.4 kpc. It is obvious that not all satellites fall onto this plane. Outliers can hamper the determination of a best-fit solution for the simple reason that they are not physically associated with the underlying population that presumably forms such a disk.

3.2. *Bootstrap Tests of Best-Fit Planes*

When fitting a plane to a set of data points, the influence of outliers can be overestimated and can yield significantly different results. However, since one cannot flag any data point as an outlier a priori, we have to use a statistical method to reliably determine a robust solution for estimating best-fit planes. We approach this problem by a bootstrap test (Efron & Tibshirani 1993). That is, we draw any possible combination of a subsample from the satellites, where we covered all possible sample sizes from 3 to all 15 companions, thus allowing us to run $\sum_{i=3}^{15}\binom{15}{i}$ different tests. For each of the 32,647 possible subsamples we performed the plane fit as described above. The resulting distribution of the normal vectors of the best-fit planes is shown in Figure 2 (*top left*), where the total of all 15 companions forms the parent sample. Since the direction of the pole is ambiguous due to the lack of actual orbit information, ODR cannot distinguish between normal vectors that are simply inverted in b and shifted by 180° in l. These points are then assigned to the complementary plane exhibiting the mirrored normal vector. The distinct peak in Figure 2 (*top left*) occurs in the direction of $l=150\overset{\circ}{.}8$ and $b=-56\overset{\circ}{.}4$, which defines a best-fit plane based on a more robust method than obtained by a single fit of all data points. The resulting Δ is 100.0 kpc. It is noteworthy that this is not a polar alignment as would be expected if the Holmberg effect also occurred in M31.

Figure 3 (*left*) shows the location of all the M31 companions and the great plane that was derived from this ODR fit comprising the entire sample of 15 satellites. The diagram is shown from a viewpoint rotated such that the great plane is seen edge-on. This great plane comprises all dEs, M32, and all dIrrs except for the transition-type dIrr/dSph PegDIG (located at a distance of 410 kpc to M31).

Although not used in the fits discussed above, we superposed the location of the Andromeda Stream (McConnachie et al. 2003) onto the diagram (Fig. 3). This stream has been shown to extend to at least $4\overset{\circ}{.}5$ southeastward of M31. The 10 fields from McConnachie et al. (2003) (error bars were omitted for clarity) are naturally aligned with respect to each other but are still located in a separate plane inclined against the best-fit plane of our analysis by approximately 7°. We did not attempt to include other features, such as And NE (Zucker et al. 2004a), since their three-dimensional position is less well known.

3.3. *Statistical Significance of the Planes*

In order to assess the statistical significance of the previously determined best-fit plane, we ran a number of additional tests. First, we generated a random sample of 15 satellites, distributed out to the maximum distance of the observed companions. The radial distribution of the random satellites was taken to follow a power law with an exponent of -2, which is a fairly good approximation of the actual radial distribution of the M31 companions and is also similar to the prediction of cosmological subhalos (Klypin et al. 1999; Moore et al. 1999; Zentner & Bullock 2003). By means of a Kolmogorov-Smirnov test it can be shown that the cumulative sample of companions is consistent with such an isothermal density distribution at 99.1%, where the most likely power-law indices fall in the range between -1.6 and -2.3 (see also Kroupa et al. 2005). The innermost satellite was, however, ignored in this procedure, since the central regions of the M31 system are known to be incompletely sampled by observations. Figure 4 shows the radial distribution of the observed satellites relative to M31. Then the entire procedure of bootstrap-fitting planes to this random distribution was carried out analogously to that of the real observed set as described in § 3.2. We determined the best-fit plane from the corresponding density maps (see Fig. 2 [*bottom panels*] for a sample) of the 32,647 combinations and calculated the respective rms distance of the 15 random points to this plane. This procedure was repeated a large number of times (on the order of 10^3) to allow us to assess the probability that the rms distance Δ originates from a random distribution and to also identify any other potential biases in our method. For the best-fit plane to the entire satellite sample of 15 companions we find a significance of 87.4%; hence, our result is robust at the 1.5 σ level. Therefore, we cannot reject the hypothesis that such a plane may result from a random distribution and thus may not have any physical meaning. Including

[2] It is often convenient to give $\boldsymbol{n}$ in its spherical parameterization, i.e., $l=\arctan(n_2/n_1)$ and $b=\arctan[n_3/(n_1^2+n_2^2)^{1/2}]$.

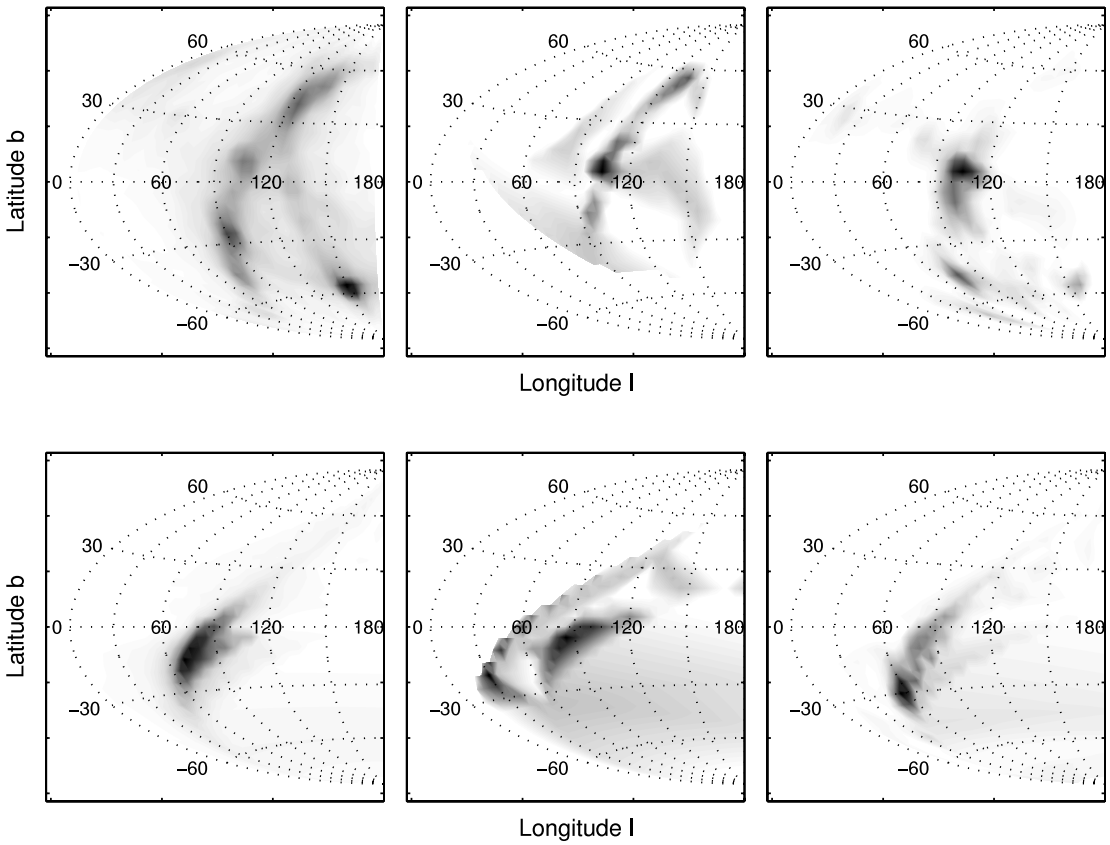

FIG. 2.—Number density distributions of the normal vectors from all bootstrap runs. The top panels are drawn from the fits to the observed galaxy sample, whereas the bottom panels show *one* sample each of the large number of tests run on a random distribution. The left panels refer to all possible fits of great planes to galaxies from the entire sample of the 15 M31 companions. The middle panels show the results of fitting only the seven dSphs. The distributions after the exclusion of the And II dSph and the inclusion of the dEs and M32 are shown in the right panels. Distinct maxima in the observed plots at ($l = 150\overset{\circ}{.}8$, $b = -56\overset{\circ}{.}4$), ($l = 107\overset{\circ}{.}1$, $b = 6\overset{\circ}{.}9$), and ($l = 102\overset{\circ}{.}6$, $b = 5\overset{\circ}{.}2$) indicate poles of the respective best-fit planes. Maxima in the random distribution do not stand out clearly and appear smeared out.

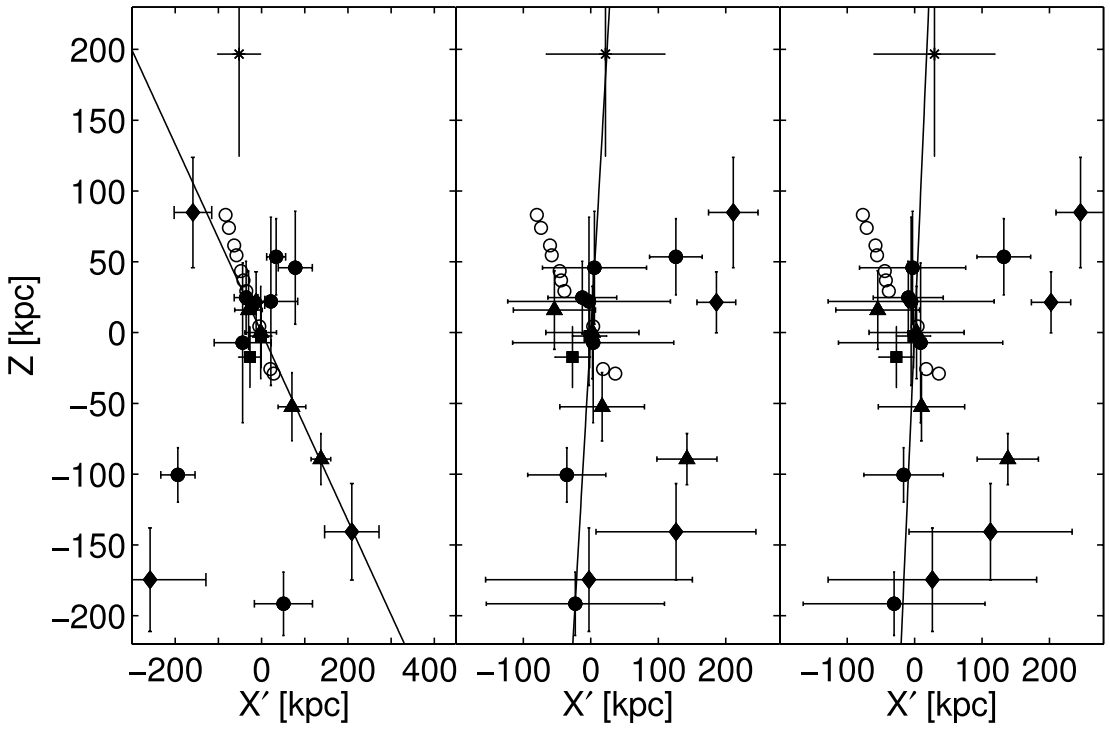

FIG. 3.—Position of the satellite galaxies shown in edge-on projections perpendicular to the best-fit planes. The left panel shows the fit to the entire dwarf sample. The middle panel illustrates the best fit to the dSph subsample. The right panel displays the rotated CS and incorporates the best fit to the combined dE/cE and dSph sample while excluding the outlier And II. The symbols are the same as in Fig. 1. Note that the horizontal error bars in these projections indicate the combined uncertainties of the X_{M31} and Y_{M31} positions. [*See the electronic edition of the Journal for a color version of this figure.*]

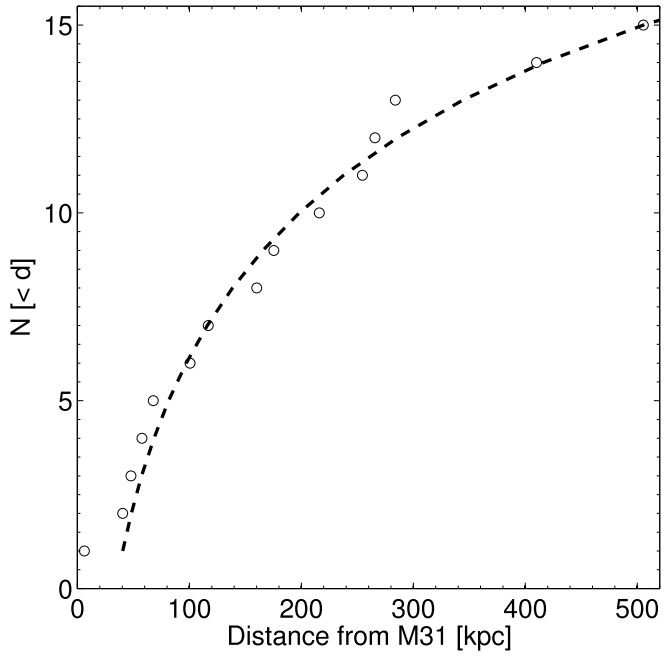

FIG. 4.—Cumulative radial distribution of the M31 satellites. The dashed line is a power law with an exponent of −2.

McConnachie et al.'s (2003) 10 fields from the Andromeda Stream in the fit routines did not alter the location of the resulting plane much. For this enlarged sample we found a normal vector of ($l = 148.^\circ5$, $b = -53.^\circ3$) with a residual rms of 78 kpc. However, an interpretation of this latter result should be taken with caution, since the sample is biased toward the stream due to the incorporation of 10 fields for one contiguous feature (i.e., the stream) versus 15 individual satellites. Hence, stating any significance will not be meaningful, as we would produce an artificially increased significance from the large number of fields.

A second test for the robustness of the fitting method employed here comprised the rotation of the real galaxy sample by pairs of random angles. The resulting data were subsequently subjected to the same fitting procedure as above, again repeated for a large number of samples. As a result, we could recover the best-fit plane rotated by the input random angles, where the scatter around the original best-fit angles amounts to approximately $5^\circ-10^\circ$. This lends further support to the results obtained with the method used here and, in addition, provides an estimate of typical uncertainties that result from the fits.

4. A POLAR PLANE OF EARLY-TYPE M31 COMPANIONS

In § 3 we analyzed the entire sample of M31 companions comprising dEs, cEs, dSphs, and dIrrs, as well as transition types such as the dIrr/dSph LGS3. Since the dSphs form the most numerous dwarf subsample in a galaxy group, and since the majority of satellite candidates of the massive Local Group galaxies are dSphs (e.g., Grebel 1999), we performed the bootstrap fit procedure including only the seven dSph satellites. It is noteworthy that, while a fit to the full sample of all M31 satellites does not yield a highly significant, unambiguous solution, the majority of dSphs lie within a plane defined by $l = 107.^\circ1$ and $b = 6.^\circ9$ (see Fig. 2, *top middle*) with an rms of $\Delta = 46$ kpc. This plane is indicated in Figure 3 (*middle*) after rotating the viewpoint by the respective longitude. Only one dSph deviates considerably from this plane: And II, located at a distance of 158 kpc to M31 and 112 kpc to the plane, where the latter value is larger than 2 σ. Excluding this obvious outlier yields a high significance (determined as above by a large number of random samples of seven satellites) of the resulting dSph plane of 99.7%, corresponding to 3 σ.

As Figure 3 (*middle*) implies, M31's close companions, the cE M32 and the dE NGC 147 (as well as the transition-type dIrr/dSph PegDIG), also lie reasonably close to the best-fit dSph plane. We may thus ask whether an improved fit would result when *all* morphologically similar galaxies are included, i.e., all galaxies of the dSph/dE/cE class. We reran the bootstrap test on this enlarged subgroup. This procedure yields a slightly different plane at $l = 102.^\circ6$, $b = 5.^\circ2$ (see the right panels of Figs. 2 and 3) with an rms of the residuals of $\Delta = 51$ kpc (without And II). As a result, the significance amounts to 98.7% (2.5 σ), again excluding the outlier And II. Hence, there is very little difference from the previous fit that included only dSphs. However, if we consider

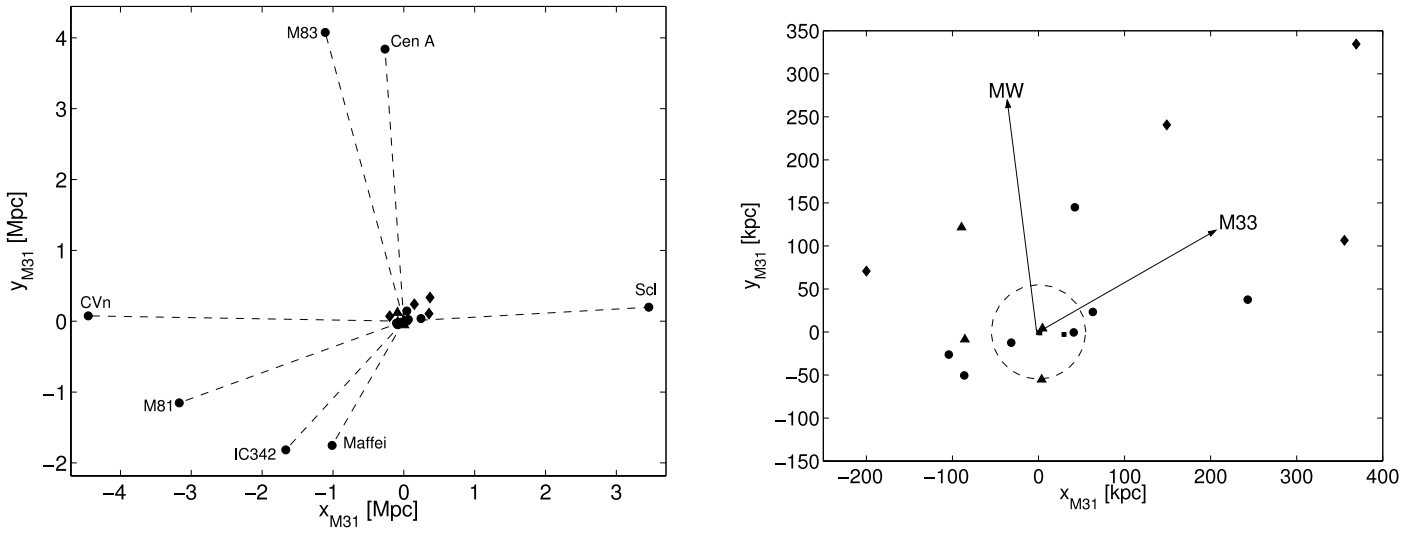

FIG. 5.—Face-on views onto M31's disk plane. *Left*: Projected location of nearby galaxy groups as given by their most luminous member. *Right*: Zoom of M31's immediate vicinity, showing its satellites. The circle designates the central 55 kpc, corresponding to the optical radius of M31's disk. Arrows indicate the direction of the Milky Way (MW) and M33. The symbols are the same as in Fig. 1. The polar great plane of M31's early-type satellites lies along an axis pointing toward the M81 group (*left*) and toward M33 (*right*). [*See the electronic edition of the Journal for a color version of this figure.*]

TABLE 2
Effects of Varying M31's Distance on the Resulting Best-fit Planes

Fit Sample	Adopted Distance to M31 (kpc)	Best-fit Plane (deg)		Significance (%)
		l	b	
All satellites (15)	760 ± 20	150.7	−56.5	86.9
	773 ± 20	150.8	−56.4	88.0
	783 ± 20	150.2	−56.2	87.1
All dSphs (7)	760 ± 20	100.3	10.9	99.1
	773 ± 20	107.1	6.9	99.7
	783 ± 20	101.9	6.5	98.6
dSphs (without And II), dEs, and M32 (10)	760 ± 20	102.7	12.1	97.8
	773 ± 20	102.6	5.2	98.7
	783 ± 20	102.8	4.8	99.2

only those galaxies whose positions seem to be in good agreement with the polar great plane of early-type companions, namely, M32, NGC 147, PegDIG, and the dSphs but excluding And II, NGC 185, and NGC 205, these nine companions lie within a thin disk with an rms distance of 16 kpc to this early-type plane.

Interestingly, the smaller Local Group spiral M33 is also directly encompassed by this great circle (its orthogonal distance to this plane being 2.8 kpc). However, it is not related to the great plane resulting from the fit to *all* M31 satellites—here M33 has a distance of 135 kpc from the plane. Moreover, while the plane comprising all of the M31 satellites is highly nonpolar (at -56°), the great plane that includes dSphs, dEs, and the cE exhibits a nearly polar alignment with an inclination of 5°–7° from M31's pole.

The most luminous, most massive globular cluster in the Milky Way, ω Cen, shares a number of properties with dwarf galaxies and is often considered to be the stripped remnant of an accreted dwarf (e.g., McWilliam & Smecker-Hane 2005; Hilker et al. 2004; Ideta & Makino 2004; and references therein). The most massive, most luminous globular clusters known in the Local Group are located in M31. One may speculate that these objects might be nuclei or bulges of stripped dwarfs; G1, for instance, also seems to exhibit a metallicity spread (Meylan et al. 2001). If so, the progenitors of these luminous clusters may also have been early-type dwarfs. We have compared the location of the two most luminous M31 globular clusters, Mayall II or G1 and B327 (van den Bergh 1968), to the location of our polar plane of early-type galaxies. Although we did not include these objects in any of the fits, we indicate in Figures 1, 3, and 5 the positions of these massive globular clusters relative to the M31 system. These clusters have an adopted distance coincident with that of M31 itself (Rich et al. 1996; Barmby et al. 2002). While G1, which is often regarded as the most luminous globular cluster of the Local Group, lies at a distance of merely 8 kpc from this polar great plane and coincides with it to within its error bars, B327 is fully encompassed by the early-type great plane.[3]

Uncertainties in the analyses presented here result not only from uncertainties in the distances to the satellites of M31 but also from the uncertainty of the distance to M31 itself. Hence, we carried out our analysis for three widely used distances to M31 from the literature. The results discussed above rely on the Cepheid distance of 773 kpc (Freedman & Madore 1990). In addition, we also adopted the mean M31 distance of 783 kpc based on several distance indicators discussed by Rich et al. (2005) and the mean distance of 760 kpc resulting from various distance indicators given by van den Bergh (1999). The formal mean uncertainties of these distance measurements are on the order of 10–20 kpc, implying that the different distances agree within their uncertainties. The results for all three M31 distances are listed in Table 2. As the values in Table 2 demonstrate, the above variation of the distance to M31 does not significantly alter our results. The statistical presence of a polar great plane prevails.

5. DISCUSSION

5.1. *The Breakup or Tidal Remnant Scenario*

As mentioned in § 1, one of the scenarios put forward to explain the Galactic polar planes suggests that the dwarf galaxies within such a plane are tidal remnants of a more massive galaxy (e.g., Kunkel 1979; Lynden-Bell 1982). We refer to this idea as scenario I. This scenario leads to the question of whether the properties of the dwarfs, in particular with respect to their stellar populations, are consistent with an origin from a single parent galaxy. We consider this question first for the Milky Way companions and then for the M31 companions.

5.1.1. *A Few Musings on the Galactic Polar Great Planes*

For the Milky Way companions it was shown that each of these dwarfs has its own unique evolutionary history that differs from other dwarfs even when they are of the same morphological type (e.g., Grebel 1997). This need not contradict an origin from a common, subsequently accreted parent but would indicate that the separation from this parent should have occurred very early on, followed by the continued evolution of the individual tidal fragments. The low metallicities of the old populations of the dSphs (see Table 1 in Grebel et al. 2003) indicate that either the parent galaxy had evolved little when its disruption occurred (supporting the view that this must have happened in ancient times) and/or the dSphs are tidal fragments of the outer, metal-poor regions of the parent.

All nearby Galactic dwarfs seem to share a common epoch of ancient star formation that is coeval within the present-day measurement accuracy (to within $\sim$1 Gyr) and is indistinguishable from the oldest age-datable stellar populations in the Milky Way (Grebel & Gallagher 2004). The SMC appears to have an old population that is several gigayears younger than the ancient star formation episodes in the other dwarfs and in the Milky Way, but more detailed data are still needed for this galaxy. For the remaining dwarfs, a common epoch of early star formation does not necessitate a common origin but lends more support to such an idea than would widely differing times for the first significant star formation.

While the *mean* metallicities of the old populations in the various dwarfs tend to differ by a few tenths of a dex, all of these

[3] Van den Bergh (1968) argues that B327 is probably the most luminous globular cluster when its reddening is properly taken into account.

galaxies also show a considerable abundance spread among their old stars. Neither property precludes a common origin from fairly metal-poor regions of a putative common progenitor.

The Galactic dwarfs follow a metallicity-luminosity relation (e.g., Grebel et al. 2003), indicating that intrinsic processes such as their own gravitational potential, and hence the ability to retain metals, played an important role in their evolution. If these dwarf galaxies are leftovers stripped from a larger satellite, they must once again have been stripped at an early time and must then have continued to form stars after this event in order to produce the observed metallicity-luminosity relation. Clearly, the Galactic dSphs are quite different from more recently formed tidal dwarfs whose departure from the metallicity-luminosity relation readily betrays their nature (e.g., Duc & Mirabel 1998).

It would seem that sustaining the extended star formation histories of the Galactic dSphs (see, e.g., Grebel & Gallagher 2004) would be difficult in low-mass tidal remnants without dark matter unless these galaxies had substantially larger baryonic masses when they condensed than the $\sim 10^5$–$10^6\ M_\odot$ derived today from their stellar content (see also the discussion in Grebel et al. [2003] and the models presented by Wang et al. [2005] and Mashchenko et al. [2005]). Other arguments against dSphs being mere tidal remnants without dark matter include the lack of substantial line-of-sight depth (Klessen et al. 2003) and extended, fairly flat radial velocity profiles (Wilkinson et al. 2004). Nonetheless, the question of dark matter in the low-mass dSphs remains to be resolved.

Whereas some merger events that are believed to have occurred several gigayears ago have left detectable tidal streams in the Milky Way—for instance, Sagittarius and possibly Monoceros, Canis Major (Ibata et al. 1994; Newberg et al. 2002, 2003; Yanny et al. 2003; Majewski et al. 2003; Martin et al. 2004), and Triangulum-Andromeda (Rocha-Pinto et al. 2004)—no ancient event has so far been identified that could be connected to the origin of the polar great planes. If these planes do indeed have a physical meaning, this unsatisfactory situation may change with the parallax and phase space information for the vast number of Milky Way stars that will be provided by the *Gaia* mission (Perryman et al. 2001). It has been suggested that the Large Magellanic Cloud may be the main part of a broken-up parent galaxy responsible for the Magellanic Stream of dwarf galaxies and simply has not yet merged with the Milky Way (e.g., Kunkel 1979). Related hypotheses propose that the precursor of today's Sgr dSph may have been deflected into its current orbit by a collision with the Large Magellanic Cloud (Zhao 1998) and that Fornax might have been stripped of its gas by an encounter with the Magellanic Stream, leading to the H I cloud excess along its inferred orbit (Dinescu et al. 2004).

The strongest evidence in favor of or against the reality of orbital planes of dwarf galaxies will come from proper-motion measurements. At present, recent measurements reveal a complex picture. Ursa Minor can be ruled out as a member of the Magellanic Stream (Piatek et al. 2005). Fornax, excluded as a stream member by the data of Piatek et al. (2002), is proposed as a likely member of the Fornax–Leo I–Leo II–Sextans–Sculptor stream by Dinescu et al. (2004). For Carina and Sculptor the situation appears to be ambiguous at present (Piatek et al. 2003; Schweitzer et al. 1995). As more and more epochs are being added, the measurements should yield a clearer picture in the coming years.

5.1.2. *A Few Musings on the M31 Polar Great Plane*

The low-mass dSph satellites of M31 are all metal-poor and show hints of metallicity spreads (e.g., Côté et al. 1999; Guhathakurta et al. 2000; Harbeck et al. 2001). However, unlike the Galactic dSphs the M31 dSphs are dominated by old populations, lacking prominent intermediate-age or even young populations (e.g., Harbeck et al. 2001, 2004). In this sense, they show a much higher degree of homogeneity than the Galactic dSphs. The two elliptical dwarfs that appear to be associated with the polar great plane show considerable enrichment, but NGC 147's globular clusters are old and metal-poor (Da Costa & Mould 1988; Han et al. 1997), and indications of a small old and metal-poor population were recently found in M32 (Alonso-García et al. 2004). As for the Milky Way companions, a putative breakup that would have produced the early-type companions of M31 would need to have occurred at very early times.

All of the gas-deficient M31 companions follow the metallicity-luminosity relation of early-type dwarfs (Grebel et al. 2003; Harbeck et al. 2005). In the remnant scenario, this would imply that they should have undergone further chemical evolution to reach a state consistent with their luminosity; hence, one may suggest that the remnants should still have contained sufficient gas to continue to form stars for a while after the breakup. If so, then again the breakup must have occurred at very early times considering the observed absence of prominent younger populations.

The cE M32 is a very interesting object in itself: it contains a black hole with a mass of a few times $10^6\ M_\odot$ (e.g., Tonry 1984; Joseph et al. 2001), it interacts with M31 (King 1962; Choi et al. 2002), and it may be the remnant of a larger elliptical galaxy (Faber 1973; Nieto & Prugniel 1987) or the bulge of a stripped early-type spiral galaxy (Bekki et al. 2001; Graham 2002). The latter is supported by the detection of what appears to be the remains of a disk in M32 (Graham 2002). This raises the intriguing possibility that M32 may be the remnant of the parent of the dwarf galaxies located in the M31 polar great plane identified in our paper. On the other hand, M32 may be associated with the giant stellar stream around M31 (Ibata et al. 2001), since it appears to be located within the stream; however, its velocity is quite different from that of the stream (Ibata et al. 2004). The stream itself seems to be on a highly radial orbit passing very close to the center of M31. Kinematic studies suggest that its progenitor may have survived until 1.8 Gyr ago (Ibata et al. 2004). Considering this and that the stream stars are metal-rich (Ibata et al. 2001), an immediate association of the stream with the dSphs seems to be ruled out.

The M31 halo differs substantially in its properties from the Galactic halo. The stellar halo appears to extend beyond 150 kpc (Guhathakurta et al. 2005), implying that many of the dwarf satellites considered in our present study are in fact moving through the stellar halo of M31. Apart from a significant old population the halo also contains metal-rich intermediate-age populations with ages in the range 6–8 Gyr that appear to account for $\sim$30% of the stellar mass (Brown et al. 2003). With approximately -0.5 dex, the mean metallicity is comparatively high (Brown et al. 2003; Durrell et al. 2004) and exceeds that of the dSph satellites by at least 1 dex in [Fe/H]. Hence, a once larger population of M31 dSph-like galaxies may have contributed to the ancient halo of M31 but was not the dominant contributor to its complex halo population structure as a whole.

The proximity of M31's massive globular clusters G1 and B327 to the plane of early-type satellites raises the question of whether these objects should also be considered as the remnants of nucleated dwarf galaxies (e.g., Meylan et al. 2001). If they originate from the same breakup event as the remainder of the dSphs, they must have undergone a different evolution. Primarily, they would then seem to have been dominated by tidal stripping and harassment from their massive host galaxy to leave a nucleus or bulge in its present, globular cluster–like form.

5.2. *The Prolate Dark Halo Scenario*

As outlined in § 1, this scenario assumes that satellites follow the dark matter distribution of the Milky Way. Polar great planes would result if the dark halo is prolate, as some authors favor for disk galaxies (e.g., Hartwick 2000; Navarro et al. 2004) and as has been suggested for our own Milky Way from the kinematics of the Sgr dwarf tidal streams (Helmi 2004).

Our finding that most of the *low-mass* satellites within 300 kpc of M31 lie within a polar great plane is consistent with this scenario and supports the view that triaxial prolate dark halos may be a common occurrence in disk galaxies.

We note, however, that the evidence for a Holmberg effect among the M31 satellites is weak. The majority of the M31 satellites are found within $|b_{\rm M31}| < 40^\circ$ of its disk (Fig. 1, *right*).

It would be highly desirable to also carry out similar studies for the satellite populations of nearby groups. While we now have distances for many of the satellites in these systems based on the tip of the red giant branch from *HST* photometry (see Karachentsev et al. 2000, 2002a, 2002b, 2003a, 2003b, 2003c for details), the uncertainties of these distances, including, in particular, those to the massive galaxies, in these groups make it difficult to reliably derive the three-dimensional galaxy distribution with sufficient accuracy for a comparable analysis.

5.3. *The Filament Scenario*

This scenario will also result in planar alignments, which would only be polar if that is the orientation of the major axis of the dark matter distribution. Both this and the preceding scenario have the advantage that they do not require a common origin of the dwarfs and permit the presence of dark matter in the satellites.

An interesting consequence of this scenario is that one may expect to find additional dwarf galaxies when following the great planes out to larger distances, since the planes should trace the location of extended cosmological filaments.

Figure 5 shows face-on views of M31's disk: in Figure 5 (*left*) we show the present-day location of several nearby galaxy groups, represented by their brightest object with distances adopted from Karachentsev (2005) and projected onto the plane of M31's disk. It is interesting to note that while the M83 and Cen A groups are located far from the polar plane spanned by Andromeda's early-type companions, the M81 group seems to almost coincide with this great plane (or filament?). Also, the extended Sculptor group and presumably the Canes Venatici I Cloud appear to be approximately oriented toward the direction of M31's polar satellite plane, albeit at larger angles. Figure 5 (*right*) shows the immediate surroundings of M31. The two arrows indicate the directions toward the Milky Way and M33. Few satellites seem to lie at the far side of M31 as seen from the Milky Way. There is no obvious filamentary structure of M31 satellites extending toward the Milky Way, but the polar plane of early-type companions clearly points toward M33, as we pointed out earlier.

6. SUMMARY

We have presented a Cartesian coordinate system that is centered on M31 and aligned with its disk. We calculated the positions of the galaxies within 500 kpc in this CS. Most (possibly all) dwarf galaxies within this radius are likely satellites of M31. We then investigated the existence of possible great planes encompassing subsets of or all of the companions. The great plane that results when trying to account for all 15 M31 companions has low statistical significance (88%) and includes many outliers. While this plane probably has no physical meaning, interestingly, the recently discovered Andromeda Stream lies close to it and is inclined with respect to it by $\sim 7^\circ$.

If we restrict our sample selection to only gas-deficient galaxies, i.e., to the dSph, dE, and the cE companions of M31, a *polar* great plane with a statistical significance of 98% results. This supports the earlier claim of the existence of such a plane by Grebel et al. (1999), which is now supported by better and more comprehensive data. M32, NGC 147, PegDIG, and even M33's position are consistent with this great plane. When excluding three deviating early-type dwarfs (And II, NGC 185, and NGC 205) as outliers from the calculation of the statistical significance, the remaining early-type galaxies lie within a mere 16 kpc of this plane, and the resulting statistical significance is 99.7% (3 σ). The plane resembles the polar great planes of satellites found around the Milky Way and also includes the more distant dIrr/dSph transition-type galaxy PegDIG and even M33. In total, this polar plane comprises 9 out of 15 M31 companions, including 8 out of 11 of its early-type dwarfs. We note that the two most luminous globular clusters in the Local Group, both of which are located in M31, are also coincident with the plane of early-type companions.

While the plane comprising all of the M31 satellites is clearly nonpolar (at -56°), the great plane of gas-deficient satellites shows a nearly polar alignment with an inclination of 6°–8° from M31's pole. We note that, in contrast to the Milky Way, the M31 companions show little evidence for a Holmberg effect. The majority of these companions are found within $\pm 40^\circ$ of M31's equator. Our findings are relatively insensitive to the adopted distance to M31 itself.

Several scenarios have been suggested to explain the existence of polar planes. A popular scenario suggests that planes originate from the breakup of larger galaxies, keeping smaller fragments in the orbit defined by the progenitor. The fragments may be pure tidal remnants devoid of dark matter. We argue that, based on the stellar populations and metallicities of both the Milky Way and the M31 satellites, such a breakup would have to have occurred very early on. A suitable parent progenitor yet needs to be identified. Since the satellites follow the luminosity-metallicity relation, they must have continued to form stars after the breakup. There is little evidence so far that the satellites are devoid of dark matter, as one would expect from unbound tidal debris. Obviously, the best test of this scenario is via proper motions and orbits. The available proper motions for Galactic dwarfs have disproved the association of certain dwarfs with polar orbital planes but may support this for others.

The prolate dark halo scenario proposes that satellites follow the dark matter distribution of the massive galaxy they are orbiting, requiring prolate dark halos to create polar great planes. The existence of polar great planes of satellites not only around the Milky Way but also around M31 would seem to support this scenario, but as noted earlier, there is little evidence for a pronounced Holmberg effect in the satellite system of M31. Ultimately, proper motions and orbits will again provide the best test of whether the planar alignments are fortuitous or physical.

The filament scenario suggests that satellites are oriented along cosmological filaments of dark and baryonic matter that is gradually accreted by massive primaries as these continue to grow in hierarchical structure formation. In this case, planar alignments are expected not only in the immediate vicinity of massive galaxies, but such filaments should extend over much larger scales. Indeed, our polar great plane of M31 satellites points toward the M81 group. On larger scales and for more distant galaxies, this scenario can be statistically tested via

weak-lensing measurements and large-galaxy surveys (e.g., Zentner et al. 2005).

A clear distinction between the different scenarios is not yet possible. We can impose constraints based on the known stellar populations and chemical properties of the satellites as discussed before. However, we also need to keep an open mind regarding other possibilities, such as that interactions and encounters between companion galaxies may have deflected some of them and altered their orbits, or that we are reading too much into potentially fortuitous planes that may be unconnected with any physical motion of the satellites. All in all, our study underlines the urgent need for orbital information, some of which may be provided by future astrometric missions. Clearly, the distribution and motion of satellites provide important tests of galaxy formation and evolution, of the importance of accretion events, of the origin and nature of dwarf galaxies, and of CDM scenarios.

We are grateful to H. Jerjen, M. Metz, and O. Gerhard for helpful discussions. We also thank S. van den Bergh and the anonymous referee for helpful comments. We acknowledge support from the Swiss National Science Foundation through grants 200021-101924/1 and 200020-105260/1.

REFERENCES

Alonso-García, J., Mateo, M., & Worthey, G. 2004, AJ, 127, 868
Armandroff, T. E., Davies, J. E., & Jacoby, G. H. 1998, AJ, 116, 2287
Armandroff, T. E., Jacoby, G. H., & Davies, J. E. 1999, AJ, 118, 1220
Barmby, P., Perrett, K. M., & Bridges, T. J. 2002, MNRAS, 329, 461
Bekki, K., Couch, W. J., Drinkwater, M. J., & Gregg, M. D. 2001, ApJ, 557, L39
Boggs, P. T., Byrd, R. H., Rogers, J. E., & Schnabel, R. B. 1992, User's Reference Guide for ODRPACK Ver. 2.01 (Boulder: NIST), http://www.boulder.nist.gov/mcsd/Staff/JRogers/papers/odrpack_guide.dvi
Boggs, P. T., & Rogers, J. E. 1990, Cont. Math., 112, 183
Brainerd, T. G. 2005, ApJ, 628, L101
Brown, T. M., Ferguson, H. C., Smith, E., Kimble, R. A., Sweigart, A. V., Renzini, A., Rich, R. M., & VandenBerg, D. A. 2003, ApJ, 592, L17
Choi, P. I., Guhathakurta, P., & Johnston, K. V. 2002, AJ, 124, 310
Côté, P., Oke, J. B., & Cohen, J. G. 1999, AJ, 118, 1645
Da Costa, G. S., & Mould, J. R. 1988, ApJ, 334, 159
Dauphole, B., Geffert, M., Colin, J., Ducourant, C., Odenkirchen, M., & Tucholke, H.-J. 1996, A&A, 313, 119
de Vaucouleurs, G. 1958, ApJ, 128, 465
———. 1959, ApJ, 129, 521
Dinescu, D. I., Keeney, B. A., Majewski, S. R., & Girard, T. M. 2004, AJ, 128, 687
Duc, P.-A., & Mirabel, I. F. 1998, A&A, 333, 813
Durrell, P. R., Harris, W. E., & Pritchet, C. J. 2004, AJ, 128, 260
Efron, B., & Tibshirani, R. J. 1993, An Introduction to the Bootstrap (London: Chapman & Hall)
Faber, S. M. 1973, ApJ, 179, 423
Freedman, W. L., & Madore, B. F. 1990, ApJ, 365, 186
Fusi Pecci, F., Bellazzini, M., Cacciari, C., & Ferraro, F. R. 1995, AJ, 110, 1664
Graham, A. W. 2002, ApJ, 568, L13
Grebel, E. K. 1997, Rev. Mod. Astron., 10, 29
———. 1999, in IAU Symp. 192, The Stellar Content of the Local Group, ed. P. Whitelock & R. Cannon (San Francisco: ASP), 17
———. 2000, in Star Formation from the Small to the Large Scale, ed. F. Favata, A. Kaas, & A. Wilson (ESA SP-445; Noordwijk: ESA), 87
Grebel, E. K., & Gallagher, J. S. 2004, ApJ, 610, L89
Grebel, E. K., Gallagher, J. S., & Harbeck, D. 2003, AJ, 125, 1926
Grebel, E. K., & Guhathakurta, P. 1999, ApJ, 511, L101
Grebel, E. K., Kolatt, T., & Brandner, W. 1999, in IAU Symp. 192, The Stellar Content of the Local Group, ed. P. Whitelock & R. Cannon (San Francisco: ASP), 447
Guhathakurta, P., Ostheimer, J. C., Gilbert, K. M., Rich, R. M., Majewski, S. R., Kalirai, J. S., Reitzel, D. B., & Patterson, R. J. 2005, Nature, submitted (astro-ph/0502366)
Guhathakurta, P., Reitzel, D. B., & Grebel, E. K. 2000, Proc. SPIE, 4005, 168
Han, M., Hoessel, J. G., Gallagher, J. S., Holtzman, J., & Stetson, P. B. 1997, AJ, 113, 1001
Harbeck, D., Gallagher, J. S., & Grebel, E. K. 2004, AJ, 127, 2711
Harbeck, D., Gallagher, J. S., Grebel, E. K., Koch, A., & Zucker, D. 2005, ApJ, 623, 159
Harbeck, D., et al. 2001, AJ, 122, 3092
Hartwick, F. D. A. 1996, in ASP Conf. Ser. 92, Formation of the Galactic Halo...Inside and Out, ed. H. Morrison & A. Sarajedini (San Francisco: ASP), 444
———. 2000, AJ, 119, 2248
Helmi, A. 2004, ApJ, 610, L97
Hilker, M., Kayser, A., Richtler, T., & Willemsen, P. 2004, A&A, 422, L9
Holmberg, E. 1969, Ark. Astron., 5, 305
Ibata, R., Chapman, S., Ferguson, A. M. N., Irwin, M., Lewis, G., & McConnachie, A. 2004, MNRAS, 351, 117
Ibata, R. A., Gilmore, G., & Irwin, M. J. 1994, Nature, 370, 194
Ibata, R., Irwin, M., Lewis, G., Ferguson, A. M. N., & Tanvir, N. 2001, Nature, 412, 49
Ideta, M., & Makino, J. 2004, ApJ, 616, L107
Joseph, C. L., et al. 2001, ApJ, 550, 668
Kang, X., Mao, S., Gao, L., & Jing, Y. P. 2005, A&A, 437, 383
Karachentsev, I. D. 2005, AJ, 129, 178
Karachentsev, I. D., & Karachentseva, V. E. 1999, A&A, 341, 355
Karachentsev, I. D., Sharina, M. E., Dolphin, A. E., & Grebel, E. K. 2003a, A&A, 408, 111
Karachentsev, I. D., et al. 2000, A&A, 363, 117
———. 2002a, A&A, 383, 125
———. 2002b, A&A, 385, 21
———. 2003b, A&A, 398, 467
———. 2003c, A&A, 404, 93
King, I. R. 1962, AJ, 67, 471
Klessen, R. S., Grebel, E. K., & Harbeck, D. 2003, ApJ, 589, 798
Klypin, A., Kravtsov, A. V., Valenzuela, O., & Prada, F. 1999, ApJ, 522, 82
Knebe, A., Gill, S. P. D., Gibson, B. K., Lewis, G. F., Ibata, R. A., & Dopita, M. A. 2004, ApJ, 603, 7
Kroupa, P., Theis, C., & Boily, C. M. 2005, A&A, 431, 517
Kunkel, W. E. 1979, ApJ, 228, 718
Kunkel, W. E., & Demers, S. 1976, R. Greenwich Obs. Bull., 182, 241
Libeskind, N. I., Frenk, C. S., Cole, S., Helly, J. C., Jenkins, A., Navarro, J. F., & Power, C. 2005, MNRAS, 363, 146
Lynden-Bell, D. 1976, MNRAS, 174, 695
———. 1982, Observatory, 102, 202
Lynden-Bell, D., & Lynden-Bell, R. M. 1995, MNRAS, 275, 429
Majewski, S. 1994, ApJ, 431, L17
Majewski, S. R., Skrutskie, M. F., Weinberg, M. D., & Ostheimer, J. C. 2003, ApJ, 599, 1082
Martin, N. F., Ibata, R. A., Bellazzini, M., Irwin, M. J., Lewis, G. F., & Dehnen, W. 2004, MNRAS, 348, 12
Mashchenko, S., Couchman, H. M. P., & Sills, A. 2005, ApJ, 624, 726
McConnachie, A. W., Irwin, M. J., Ibata, R. A., Ferguson, A. M. N., Lewis, G. F., & Tanvir, N. 2003, MNRAS, 343, 1335
McWilliam, A., & Smecker-Hane, T. A. 2005, ApJ, 622, L29
Meylan, G., Sarajedini, A., Jablonka, P., Djorgovski, S. G., Bridges, T., & Rich, R. M. 2001, AJ, 122, 830
Moore, B., Ghigna, S., Governato, F., Lake, G., Quinn, T., Stadel, J., & Tozzi, P. 1999, ApJ, 524, L19
Navarro, J. F., Abadi, M. G., & Steinmetz, M. 2004, ApJ, 613, L41
Newberg, H. J., et al. 2002, ApJ, 569, 245
———. 2003, ApJ, 596, L191
Nieto, J.-L., & Prugniel, P. 1987, A&A, 186, 30
Palma, C., Majewski, S. R., & Johnston, K. V. 2002, ApJ, 564, 736
Perryman, M. A. C., et al. 2001, A&A, 369, 339
Piatek, S., Pryor, C., Bristow, P., Olszewski, E. W., Harris, H. C., Mateo, M., Minniti, D., & Tinney, C. G. 2005, AJ, 130, 95
Piatek, S., Pryor, C., Olszewski, E. W., Harris, H. C., Mateo, M., Minniti, D., & Tinney, C. G. 2003, AJ, 126, 2346
Piatek, S., et al. 2002, AJ, 124, 3198
Rich, R. M., Corsi, C. E., Cacciari, C., Federici, L., Fusi Pecci, F., Djorgovski, S. G., & Freedman, W. L. 2005, AJ, 129, 2670
Rich, R. M., Mighell, K. J., Freedman, W. L., & Neill, J. D. 1996, AJ, 111, 768
Rocha-Pinto, H. J., Majewski, S. R., Skrutskie, M. F., Crane, J. D., & Patterson, R. J. 2004, ApJ, 615, 732
Sales, L., & Lambas, D. G. 2004, MNRAS, 348, 1236
Schweitzer, A. E., Cudworth, K. M., & Majewski, S. R. 1997, in ASP Conf. Ser. 127, Proper Motions and Galactic Astronomy, ed. R. M. Humphreys (San Francisco: ASP), 103

Schweitzer, A. E., Cudworth, K. M., Majewski, S. R., & Suntzeff, N. B. 1995, AJ, 110, 2747
Tonry, J. L. 1984, ApJ, 283, L27
van den Bergh, S. 1968, Observatory, 88, 168
———. 1999, A&A Rev., 9, 273
Wang, X., Woodroofe, M., Walker, M. G., Mateo, M., & Olszewski, E. 2005, ApJ, 626, 145
Wilkinson, M. I., Kleyna, J. T., Evans, N. W., Gilmore, G. F., Irwin, M. J., & Grebel, E. K. 2004, ApJ, 611, L21
Yanny, B., et al. 2003, ApJ, 588, 824
Zentner, A. R., & Bullock, J. S. 2003, ApJ, 598, 49
Zentner, A. R., Kravtsov, A. V., Gnedin, O. Y., & Klypin, A. A. 2005, ApJ, 629, 219
Zhao, H. 1998, ApJ, 500, L149
Zucker, D. B., et al. 2004a, ApJ, 612, L117
———. 2004b, ApJ, 612, L121

Note added in proof.—After our paper appeared on astro-ph, a second, similar study was posted there and subsequently published (A. W. McConnachie & M. J. Irwin, MNRAS, 365, 902 [2006]). These authors analyzed the distribution of M31's satellite distribution in a coordinate system similar to the system presented here. They also claim the existence of numerous possible candidate streams and suggest that most of these streams may be chance alignments.